Journal of Mines, Metals and Fuels, *71(12C): 90-101; 2023. DOI: 10.18311/jmmf/2023/47273*

Print ISSN : 0022-2755

Journal of Mines, Metals and Fuels

Contents available at: *www.informaticsjournals.com/index.php/jmmf*

Exploring the Electronic Properties of 4,6-dimethyl-2H-chromen-2-one Substitute Coumarin Derivative via DFT Analysis

A. L. Latha[1,2], Ramani Sudha[2], Misbhahuddin khan[3], Lohit[4], Radha Rammohan Shanthanam[2], Lohit Naik[4], Yin Yao[5], Yury Kapelyushin[6], Charles Mbohwa[7], and U. Mahaboob Pasha[2,7]

[1]*Government First Grade College for Women, Vijayanagar, Mysore - 570032, Karnataka, India*
[2]*Presidency University, Bangalore - 560064, Karnataka, India*
[3]*Government College for Women, Kolar 563101, Karnataka, India*
[4]*Christ University, Bangalore - 560026, Karnataka, India; Lohitishwar.naik@christuniversity.in*
[5]*Electron Microscope Unit, Mark Wainwright Analytical Centre, UNSW Sydney, Sydney, New South Wales, 2052, Australia*
[6]*Faculty of Materials Science and Metallurgy Engineering, South Ural State University (National Research University), Prospekt Lenina, 76, Chelyabinsk, Chelyabinsk Oblast - 454080, Russia*
[7]*College of Science Engineering and Technology, University of South Africa, Pretoria, South Africa*

Abstract

In this study, we investigated the photophysical properties of 1H-imidazole substituted coumarin derivatives, specifically 4-((2-(1H-imidazol-1-yl)-1-(2-oxo-2H-chromen-3-yl)ethoxy)methyl)-6-methyl-2H-chromen-2-one (2HOE), using Density Functional Theory (DFT). The optimized bond lengths, angles, and dihedral angles of 2HOE were estimated with the DFT-B3LYP-6-311G basis set. The calculated crucial parameters such as the highest occupied molecular orbital and lowest unoccupied molecular orbital gap, solvation energy, ionization potential, electron affinity, chemical hardness, electron chemical potential, electronegativity, and global electrophilicity in different mediums to gain insights into the compound's behavior. Additionally, we estimated the molecular electrostatic potential map, total electron density, and electrostatic potential of the 2HOE molecule to study its nucleophilic and electrophilic regions. Understanding the structural, electronic, and optical properties of this compound provides valuable insights into its behavior across various mediums, with significant implications for potential biological applications.

Keywords: *Coumarin Derivative, FMO, MESP, Mulliken, UV-Vis*

1.0 Introduction

1H-imidazole substituted coumarin derivatives represent a promising class of compounds with significant potential for biological applications. Coumarins, known for their diverse pharmacological properties, are fused benzopyrone structures found abundantly in nature and have garnered attention for their various therapeutic benefits, including anticancer, antimicrobial, antioxidant, and anti-inflammatory activities. The

**Author for correspondence*

incorporation of 1H-imidazole moieties into coumarin structures enhances their biological activities and introduces new functionalities that can potentially target specific biological pathways and molecular targets[1-3].

The synthesis of 1H-imidazole substituted coumarin derivatives involves strategic modifications to the coumarin scaffold, often through synthetic methods such as condensation reactions or direct substitution of imidazole rings onto the coumarin core. These modifications aim to optimize pharmacological properties such as bioavailability, solubility, and target specificity, crucial for their application in biological systems[4-7]. The biological activities of 1H-imidazole substituted coumarin derivatives are varied and promising. They have shown potential as anticancer agents by targeting key enzymes involved in cancer cell proliferation and apoptosis pathways. Additionally, their antimicrobial properties make them candidates for combating infectious diseases caused by bacteria, fungi, and parasites. Moreover, these derivatives exhibit antioxidant effects, which can protect cells from oxidative stress and inflammation, contributing to their potential therapeutic applications in treating chronic diseases[8-11]. The structural diversity and versatility of 1H-imidazole substituted coumarin derivatives also make them valuable tools in medicinal chemistry and drug discovery. By understanding their structure-activity relationships and mechanisms of action, researchers can tailor these compounds to specific biological targets, optimizing their efficacy and minimizing potential side effects[12,13]. The 1H-imidazole substituted coumarin derivatives represent a promising avenue for the development of novel therapeutic agents with applications across various biomedical fields. Their multifaceted pharmacological activities and structural versatility underscore their potential to address current challenges in healthcare, offering new opportunities for advancing treatment modalities and improving patient outcomes[14].

In view of the above, 1-Aza-Coumarin-Linked Miconazole derivatives represent a promising class of compounds with multifaceted pharmacological attributes. In view of the above discussion, in the present work 3-(1-hydroxy-2-(1H-imidazol-1-yl) ethyl)-2H-chromen-2-one is selected and studied the their photophysical and chemical properties using DFT method.

2.0 Computational Methods

The 1-Aza-Coumarin-Linked Miconazole derivatives, namely 7 4-((2-(1H-imidazol- 1-yl) -1-(2-oxo-2H-chromen-3-yl) ethoxy)methyl)-6- methyl-2H-chromen-2-one (2HOE) is selected from the literature[15] and the molecular structure of the 2HOE was given in Figure 1.

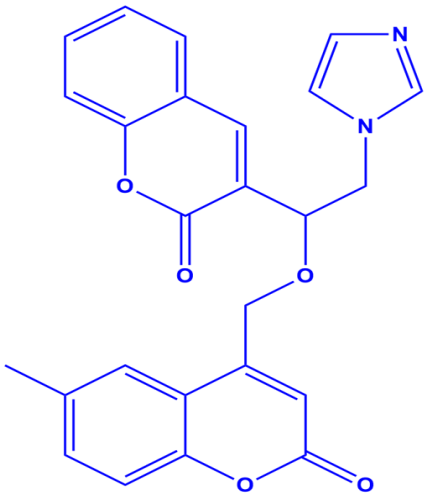


Figure 1. Molecular structure of the 2HOE molecule.

The structural and theoretical analyses of 2HOE were conducted using GaussView 5.0 and Gaussian 09 W software packages[16]. The optimization of 2HOE geometry was initially performed via Density Functional Theory (DFT) employing the B3LYP functional and 6-311G basis set. Subsequently, various theoretical investigations were carried out, encompassing atomic charge distribution in the ground state, Time-Dependent DFT (TD-DFT) analysis in the excited state, thermodynamic properties, structural properties, and optical properties. The DFT method B3LYP/6-311G was utilized for these analyses. Additionally, frontier molecular orbital analysis of the molecule was conducted both in vacuum and in a liquid phase environment. This comprehensive approach enabled a thorough exploration of 2HOE's electronic structure, thermodynamic behavior, and optical characteristics, shedding light on its potential applications and informing further research endeavors. Thermodynamic parameters including Self-Consistent Field (SCF) energy, enthalpy, entropy, dipole moment, zero-point vibrational energy,

heat capacity, and rotational constants were computed to elucidate 2HOE's energetic and structural attributes. Moreover, the energy levels of the HOMO and LUMO were examined across different mediums, allowing for the assessment of key molecular properties, such as ionization ability, electron affinity, chemical hardness, and electrophilic index. Additionally, Density Functional Theory (DFT) was employed to analyze the Total Electron Density (TED) surface mapping, Electrostatic Potential (ESP), and Molecular Electrostatic Potential (MEP), contour mapping of 2HOE in both vacuum and solvent mediums, offering insights into its molecular interactions.

3.0 Results and Discussion

3.1 Structure and Geometric Properties

The structural design of 2HOE was initially generated in GaussView-5 and subsequently optimized using Gaussian 09 software. The optimization process, conducted with the "opt" keyword, utilized the B3LYP functional and the 6-311G basis set[17]. Starting from standard parameters, the Gaussian program iteratively minimized the geometry to identify the configuration with the lowest energy, resembling the molecular structure at its energy minimum. The resulting optimized molecular geometries of 2HOE are depicted in Figure 2, providing visual representation of the molecule's conformational characteristics.

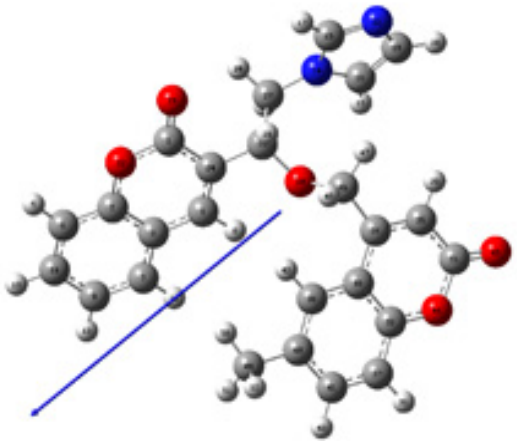


Figure 2. Optimised molecular geometry of the 2HOE molecule.

The structural parameters of the molecule 4-((2-(1H-imidazol-1-yl)-1-(2-oxo-2H-chromen-3-yl)ethoxy)methyl)-6-methyl-2H-chromen-2-one, calculated using DFT/B3LYP/6-311G, provide a detailed understanding of its geometric configuration. The bond lengths, bond angles, and dihedral angles reveal important aspects of the molecule's three-dimensional structure, crucial for understanding its reactivity and interactions. The value bond lengths, bond angles, and dihedral angles are given in Table 1. The bond lengths in the molecule show a range of values, indicating the diversity of chemical environments around the atoms. Notable bond lengths include 1.233 Å for the C1-O23 double bond and 1.413 Å for the C1-O22 single bond. The C1-C24 and C24-C25 bonds measure 1.352 Å and 1.546 Å, respectively, reflecting typical single bonds between carbon atoms. The nitrogen-carbon bonds, such as N14-C27 at 1.459 Å and N14-C15 at 1.382 Å, are within expected ranges for single and double bonds. Additionally, the O30-C46 bond length is 1.464 Å, characteristic of a single bond between carbon and oxygen. These bond lengths indicate typical bonding patterns within the molecule. The bond angles provide insight into the planar and non-planar regions of the molecule. The O22-C1-O23 angle is 117.85°, slightly less than the ideal 120° for sp^2 hybridized carbon, suggesting minor distortions due to nearby substituents. The C24-C25-C27 angle is 111.09°, typical of a tetrahedral arrangement around sp3 hybridized carbon, while the C25-O30-C46 angle of 115.69° indicates some strain or steric effects. These angles reveal the orientation of different parts of the molecule relative to each other, influencing its overall shape.

The dihedral angles describe the relative spatial arrangement of atoms and the intersection of different planes within the molecule. Significant dihedral angles include C1-C24-C25-O30 at 166.70°, nearly planar, indicating extended conjugation. The C24-C25-C27-N14 angle is 177.68°, almost planar, suggesting a stable conformation with minimal torsional strain. The C25-O30-C46-C34 angle is 175.01°, also nearly planar, indicating extended conjugation or alignment. The H39-C35-C31-O44 angle is perfectly planar at 179.44°, reinforcing the idea of extended conjugation in this region. These dihedral angles show how different parts of the molecule are twisted relative to each other, which is important for understanding its electronic

Table 1. Estimation of Bond length (Å), Bond angle (°) and dihedral angle of HCE using DFT/B3LYP/6-311G

Atoms	Bond length (Å)	Atoms	Bond Angle (°)	Atoms	Dihedral Angle (°)
1C-23O	1.233	O22-C1-O23	117.85	C1-C24-C25-O30	166.70
1C-22O	1.413	O22-C1-C24	116.45	C24-C25-C27-N14	177.68
6C-H5	1.079	C24-C25-C27	111.09	C27-C25-O30-C46	104.76
1C-24C	1.352	C25-C27-N24	112.89	C25-O30-C46-C34	175.01
24C-4C	1.352	C25-O30-C36	115.69	O30-C46-C34-C35	108.12
24C -25C	1.546	O30-C46-C34	107.71	H39-C35-C31-O44	179.44
25C-27C	1.544	N14-C16-C18	105.48		
27C-H28	1.088	C16-C18-N21	110.21		
27C-N14	1.459	C25-O30-C46	115.96		
14N-15C	1.382	O30-C46-C34	107.45		
15C-N21	1.328	H50-C49-C40	111.39		
21N-18C	1.346	C32-O44-C31	122.11		
18C-16C	1.374	O44-C31-O45	117.90		
16C-N14	1.399				
25C-O30	1.460				
O30-46C	1.464				
46C-34C	1.506				
31C-O44	1.422				
31C-O45	1.206				
40C-49C	1.512				

distribution and reactivity. The structural parameters of 2HOE molecules highlight a combination of planar and non-planar regions with various bond lengths and angles reflecting its complex structure. The bond lengths indicate typical single and double bonds, while the bond angles suggest some strain or steric hindrance in specific areas. The dihedral angles reveal significant planarity in certain regions, indicative of extended conjugation, potentially affecting the molecule's electronic properties. These parameters provide a basis for understanding the molecule's stability, reactivity, and behavior in different chemical environments[18].

The Mulliken atomic charge distributions[19] of each atomic site in 2HOE were investigated using DFT with the B3LYP/6-311G method in three different environments: vacuum, hexene, and dimethyl sulfoxide solvents (DMSO). Table 2 presents the Mulliken charge distribution of each atom in 2HOE different mediums, highlighting the solvent influences. Figures 3 and 4 were shows graphically illustrates of the variation in charge distribution across

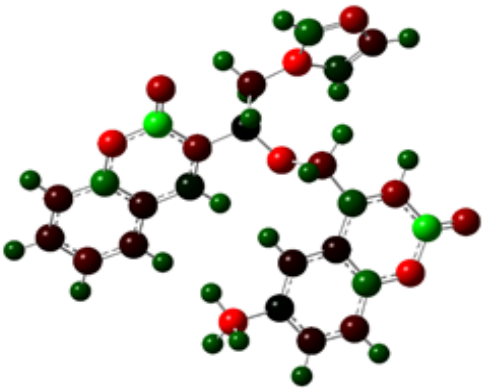


Figure 3. Mulliken charge distribution on the 2HOE molecule.

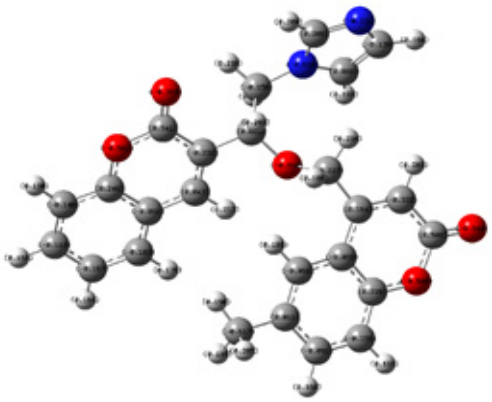


Figure 4. A statistical representation of Mulliken charge distribution on the 2HOE molecule in the gas phase.

molecules. The Mulliken atomic charges for the molecule 4-((2-(1H-imidazol-1-yl)-1-(2-oxo-2H-chromen-3-yl) ethoxy)methyl)-6-methyl-2H-chromen-2-one were calculated using DFT/B3LYP/6-311G in three different environments: vacuum, hexane, and DMSO. These atomic charges reveal important insights into the electronic distribution within the molecule, which influences its reactivity, intermolecular interactions, and stability. In general, the charges vary across different media, with the most pronounced changes observed in the polar solvent DMSO. For instance, the carbonyl oxygens (22O and 23O) exhibit significant negative charges, which decrease in magnitude from vacuum to DMSO, indicating stabilization through solvation. Specifically, the charge on 22O changes from -0.502 in vacuum to -0.363 in DMSO. The nitrogen atoms in the imidazole and quinoline rings (14N and 21N) also show substantial negative charges, with 14N being more negative than 21N. The magnitude of these charges decreases in polar solvents, suggesting interactions with the solvent molecules that stabilize the charges. For example, the charge on 14N changes from -0.628 in vacuum to -0.489 in DMSO.

Hydrogen atoms attached to carbons, such as 5H and 8H, exhibit positive charges that increase in polar solvents, indicating enhanced polarization of C-H bonds. This trend suggests that polar solvents increase the partial positive charge on hydrogen atoms, as seen with 5H changing from 0.191 in vacuum to 0.330 in DMSO. In vacuum, the charges are relatively moderate, reflecting the intrinsic electron distribution without external influence. In hexane, a non-polar solvent, there are slight changes in charge distribution compared to vacuum, indicating some interaction with the solvent. In DMSO, a polar solvent, significant changes in atomic charges are observed, with an increase in positive charges on hydrogen atoms and a decrease in negative charges on electronegative atoms (oxygen and nitrogen). This highlights strong solvation effects that stabilize the charges. Specific observations include carbon atoms connected to oxygen or nitrogen (like 1C and 2C), which have higher positive charges in DMSO compared to vacuum, reflecting stabilization by the polar solvent. Hydrogen atoms generally show increased positive charges in hexane and DMSO compared to vacuum, aligning with increased polarization in the presence of solvents. Nitrogen atoms, especially 14N, carry substantial negative charges that become less negative in DMSO, underscoring solvation effects. Oxygen atoms consistently exhibit high negative charges, with magnitudes decreasing in polar solvents, further indicating strong solvation interactions. The Mulliken atomic charges reveal that in polar solvents like DMSO, there is a clear trend of charge stabilization and redistribution, which is crucial for understanding the molecule's behavior in different media. These shifts in electron density suggest enhanced reactivity in polar environments due to the stabilization of charged regions, providing valuable insights for predicting the molecule's behavior in biological systems or during synthesis and application in various solvent conditions.

The thermodynamic parameters serve as pivotal indicators in understanding chemical processes. Utilizing Density Functional Theory (DFT), we investigated

Table 2. Mulliken atomic charges by DFT/ B3LYP/6-311G in vacuum and solvent medium

Atom label	Vacuum	Hexene	DMSO
1C	0.541	0.636	0.680
2C	0.249	0.345	0.388
3C	-0.091	0.004	0.048
4C	0.041	0.137	0.180
5H	0.191	0.286	0.330
6C	-0.139	-0.044	0.000
7C	-0.104	-0.009	0.035
8H	0.215	0.310	0.354
9C	-0.168	-0.073	-0.029
10C	-0.113	-0.018	0.026
11H	0.175	0.271	0.314
12H	0.164	0.260	0.303
13H	0.167	0.262	0.306
14N	-0.628	-0.533	-0.489
15C	0.206	0.301	0.345
16C	0.088	0.184	0.227
17H	0.209	0.304	0.348
18C	-0.139	-0.043	0.000
19H	0.199	0.294	0.338
20H	0.184	0.279	0.323
21N	-0.370	-0.275	-0.231
22O	-0.502	-0.406	-0.363
23O	-0.363	-0.268	-0.224
24C	-0.230	-0.135	-0.091
25C	-0.001	0.095	0.138
26H	0.204	0.299	0.343
27C	-0.157	-0.062	-0.018
28H	0.232	0.328	0.371
29H	0.201	0.297	0.340
30O	-0.517	-0.422	-0.378

31C	0.499	0.595	0.638
32C	0.225	0.320	0.364
33C	-0.061	0.034	0.078
34C	0.165	0.260	0.304
35C	-0.322	-0.226	-0.183
36H	0.184	0.280	0.323
37C	-0.163	-0.067	-0.024
38C	-0.054	0.042	0.085
39H	0.203	0.299	0.342
40C	-0.021	0.074	0.118
41C	-0.086	0.009	0.053
42H	0.193	0.288	0.332
43H	0.163	0.258	0.302
44O	-0.506	-0.411	-0.367
45O	-0.344	-0.248	-0.205
46C	-0.228	-0.132	-0.089
47H	0.232	0.328	0.371
48H	0.189	0.284	0.328
49C	-0.603	-0.508	-0.464
50H	0.192	0.287	0.331
51H	0.204	0.299	0.343
52H	0.197	0.292	0.336

various statistical thermodynamic properties of 2HOE at a temperature of 298.15 K and 1atm pressure. The DFT/B3LYP/6-311G method facilitated the determination of translational, rotational, vibrational, total, and nuclear repulsion energies, as well as zero-point vibrational energy and other statistical thermodynamic parameters such as entropy (S), rotational constants, molecular capacity at constant volume, and dipole moment. These findings, outlined in Table-3, provide essential insights for further exploration of 2HOE's molecular behavior and pave the way for comprehensive studies on this compound[20].

The thermodynamic parameters of the molecule 4-((2-(1H-imidazol-1-yl)-1-(2-oxo-2H-chromen-3-yl) ethoxy)methyl)-6-methyl-2H-chromen-2-one, estimated using DFT theory with the B3LYP/6-311G (d,p) basis set, provide comprehensive insights into its stability, molecular behavior, and interaction with its environment. The energy components calculated include translational, rotational, and vibrational energies. The translational and rotational energies are both 0.871 kcal mol^{-1}, which are relatively small compared to the vibrational energy of 94.458 kcal mol^{-1}. The total energy sums up to 96.200 kcal mol^{-1}, indicating that the vibrational contribution

Table 3. Calculated thermodynamic parameters of 2HOE with DFT theory using the B3LYP/6-311G (d, p) basis set

Parameters	Values
Energy	
Translational (kcal mol^{-1})	0.871
Rotational (kcal mol^{-1})	0.871
Vibrational (kcal mol^{-1})	94.458
Total	96.200
Nuclear repulsion energy (Hartree's)	1328
Zero-point vibrational energy (kcal mol^{-1})	95.285
Entropy, S (Cal/Mol-Kelvin)	122.43
Molecular capacity of constant volume (cal mol^{-1} k^{-1})	3.231
Translational	1.987
Rotational	35.229
Vibrational	51.325
Total	88.541
Rotational constants (GHz)	
A	1.231
B	0.176
C	0.134
Dipole moment (D)	10.291

dominates the molecule's energy profile. This suggests that vibrational modes, which involve movements of atoms relative to each other, are significant in defining the molecule's thermodynamic behaviour.

The nuclear repulsion energy is given as 1328 Hartree's, a measure of the repulsive forces between positively charged nuclei in the molecule. This high value reflects the intrinsic stability due to the balance of repulsive and attractive forces within the molecule's structure. The Zero-Point Vibrational Energy (ZPVE) is calculated to be 95.285 kcal mol^{-1}. ZPVE represents the lowest possible energy that the molecule can possess and is crucial for understanding its ground state properties. This value is close to the total vibrational energy, emphasizing the significant role of vibrational states even at absolute zero temperature. The entropy (S) of the molecule is 122.43 cal/mol-Kelvin, which indicates the degree of disorder or randomness in the system. A higher entropy value is associated with greater molecular disorder, which can be linked to the molecule's flexibility and the number of accessible microstates. The molecular capacity at constant volume (Cv) is 3.231 cal/mol-Kelvin. This parameter provides insight into the amount of energy required to raise the temperature of the molecule by one degree Kelvin at constant volume. The individual contributions to Cv from translational, rotational, and vibrational motions are 1987, 35.229, and 51.325 cal/mol-Kelvin, respectively. The dominant contribution from vibrational motion again highlights the significance of vibrational modes in the thermodynamic behavior of the molecule. Rotational constants (A, B, and C) are 1.231 GHz, 0.176 GHz, and 0.134 GHz, respectively. These constants are crucial for understanding the rotational motion of the molecule and are related to the moments of inertia around the principal axes. They provide insights into the molecule's shape and the distribution of mass within it. The dipole moment is calculated to be 10.291 D, indicating a substantial separation of positive and negative charges within the molecule. A high dipole moment suggests strong interactions with electric fields and other polar molecules, which can influence solubility, reactivity, and intermolecular interactions. The calculated thermodynamic parameters of the molecule highlight the predominance of vibrational energy, significant nuclear repulsion, substantial entropy, and a high dipole moment. These factors collectively suggest that the molecule is thermodynamically stable, with notable vibrational activity and strong interactions with its environment. This detailed thermodynamic profile is essential for predicting the molecule's behavior in various chemical and physical processes.

3.2 Frontier Molecular Orbitals (FMO) and Quantum Chemical Calculation

The FMO enables recognition of the electron charge

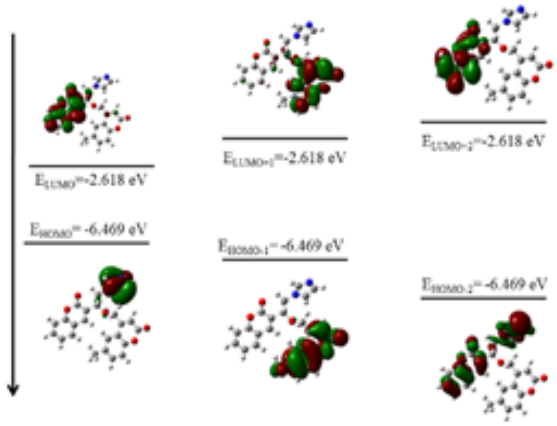


Figure 5. 3D representation of frontier molecular orbital of 2HOE in DMSO using the DFT method.

transfer between the donor and acceptor groups via the π-conjugate system. The HOMO (electron-donating) is directly associated with the ionization potential, while the LUMO (electron-accepting) is associated with the electron affinity of the compound. Plotting the FMO helps us gain deeper insights into the nature of the chemical structure and reactions of the molecule[8,21]. HOMO, HOMO-1, and HOMO-2 are orbitals that exhibit π-bonding symmetry, whereas LUMO, LUMO+1, and LUMO+2 are molecular orbitals showing π* antibonding symmetry. Figure 6 presents a 3D representation of the frontier molecular orbitals in different media using the DFT method with the B3LYP functional and the 6-311G basis set, where the green area indicates the positive region and the red area shows the negative region of the molecular orbital.

The energy gap (E_g) has been analyzed using the equation (1) provided below, which gives the energy gap (E_g) between HOMO and LUMO. The E_g in the DMSO medium shows the largest energy gap of 5.464 eV, the energy gap between HOMO-1 and LUMO+1 is 6.224 eV, and the E_g between HOMO+2 and LUMO-2 is 6.978 eV.

It is important to study the global chemical reactivity descriptors (GCRD) properties[22] to understand more about the stability and reactivity of synthesized compounds. The GCRD parameters like chemical hardness (η=(IP-EA)/2), electronegativity (χ=(IP+EA)/2), chemical potential (μ=-χ), chemical softness (S=1/2η) and electrophilicity index (ω=μ²/2η) were calculated from E_{HOMO} and E_LUMO values, where, ionization potential, IP=-E_{HOMO} and electron affinity, EA=-E_{LUMO}.

From Figure 6, it is observed that the LUMO electron cloud is mainly distributed across the coumarin molecule, while the HOMO electron cloud is partially located on the 1-methyl-1H-imidazole. The GCRD parameters for all the molecules are provided in Table 4.

The study of global chemical reactivity descriptors (GCRD) provides valuable insights into the stability and reactivity of the synthesized molecule 4-((2-(1H-imidazol-1-yl)-1-(2-oxo-2H-chromen-3-yl)ethoxy) methyl)-6-methyl-2H-chromen-2-one. The key GCRD parameters calculated for this molecule include chemical hardness (η), electronegativity (χ), chemical potential (μ), chemical softness (S), and electrophilicity index (ω). The chemical hardness (η) is 1.987 eV, indicating that the molecule is relatively stable and resistant to changes in its electron distribution. The electronegativity (χ) of 4.691 eV suggests a strong tendency to attract electrons, highlighting its potential reactivity in electrophilic reactions. The chemical potential (μ) is -4.691eV, reinforcing the molecule's stability and low tendency to lose electrons. Furthermore, the chemical softness (S) is 0.252, which indicates moderate reactivity, suggesting that the molecule can participate in chemical reactions but is not extremely reactive. The electrophilicity index (ω) is 5.538 eV, signifying a significant electrophilic nature and the molecule's readiness to accept electrons from nucleophiles. Additionally, the ionization potential (IP) of 6.677 eV and electron affinity (EA) of 2.704 eV indicate the molecule's stability and moderate tendency to gain electrons. The GCRD parameters for 4-((2-(1H-imidazol-1-yl)-1-(2-oxo-2H-chromen-3-yl) ethoxy)methyl)-6-methyl-2H-chromen-2-one reveal that

Table 4. Global electrochemical reactivity descriptor parameter for all synthesized molecules

E_{HOMO} (eV)	E_{LUMO} (eV)	ΔE (eV)	IP (eV)	EA (eV)	h (eV)	c (eV)	μ (eV)	s (eV^{-1})	ω (eV)
-6.677	-2.704	3.973	6.677	2.704	1.987	4.691	-4.691	0.252	5.538

it is relatively stable with moderate reactivity. The molecule has a high tendency to attract electrons, significant electrophilic character, and a moderate ability to deform its electron cloud in response to external influences, making it suitable for reactions with nucleophiles.

3.3 Electrostatic Potential (ESP), Total Electron Density (TED) and Molecular Electrostatic Potential (MESP) Studies

The three-dimensional mappings of electrostatic potential, total electron density, and molecular electrostatic potential were generated using DFT theory with the B3LYP functional and 6-311+G basic set. These mappings of 2HOE derivative structure are analysed through surface contouring in Gaussian-09.

3.3.1 ESP of 2HOE Molecule

The electrostatic Potential (ESP) illustrates the interaction energy between the molecule's electrons and point positive charges near nuclei. Figure 6 displays the ESP mapping of the 2HOE molecule, indicating energy ranging from -0.512 eV to 0.512 eV in vacuum and from -0.329 eV to 0.329 eV in DMSO solvent. Notably, sites O29 and O31 exhibit the most negative potential values of -0.312 eV and -0.303 eV, respectively, in vacuum and these areas are highlighted in red. Additionally, the region encompassing 26N and 19N shows potential values of 0.133 eV and 0.102 eV (yellow) in vacuum.

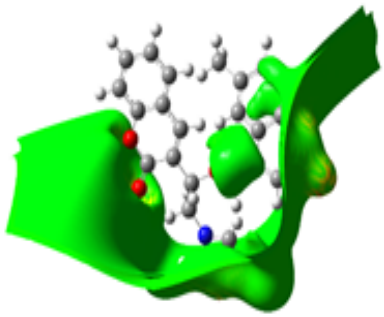


Figure 6. Electrostatic potential mapping of 2HOE molecule in vacuum.

3.3.2 TED of 2HOE Molecule

DFT provides a theoretical framework to estimate this Total Electron Density (TED). Electron density

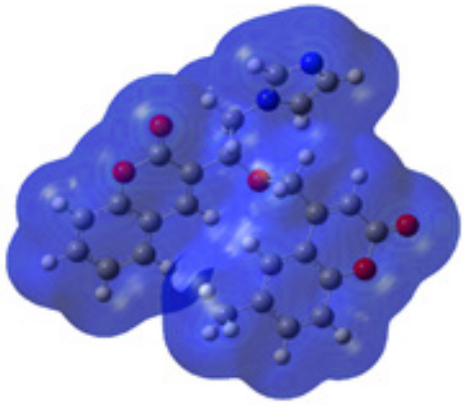


Figure 7. Total electron density mapping of 2HOE molecule in vacuum.

mapping uses in analysing the molecule's shape, charge, and delocalization, offering insights into its chemical reactivity. Figure 7 illustrates the TED mapping of 2HOE in vacuum, indicating electron densities of ± $4.148x10^{-2}$ Hartrees (± 0.011 eV) in vacuum. The electron density shows, a uniform distribution across the molecule's surface. These results help in understanding various properties of a system, such as chemical bonding, interactions and other important electronic properties.

3.3.3 MEP of 2HOE Molecule

The Molecular Electrostatic Potential (MESP) mapping, conducted using DFT/B3LYP/6-311G in various solvents, depicts potential distribution can be observed by colour

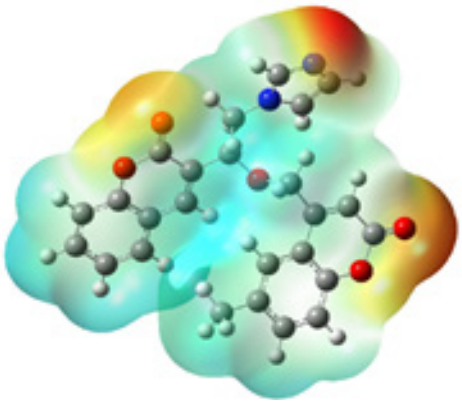


Figure 8. Molecular electrostatic potential mapping of 2HOE molecule in vacuum. .

code. Figure 8 presents the MESP mapping of 2HOE in vacuum and DMSO, displaying contour values ranging from -6.965 eV to 6.965 eV in vacuum. The red regions, primarily surrounding 22O, 23O, 44O and 45O signify lower energy levels, making these atoms susceptible to nucleophilic attacks as electron acceptors. Conversely, the methyl group attached to carbon atom 20 C (atoms 20H, 23H, and 25H) displays maximum positive charge (blue region), rendering them susceptible to electrophilic attacks as electron donors. Yellow colour around 25N and 16N represents nucleophilic sites. Neutral (green) region is widespread across the molecule, particularly on benzene ring structures and certain carbon atoms. Positive charge (light blue) is observed at the position of hydrogen indicating its role as an electron-donator[23].

4.0 Conclusion

This study has successfully employed a computational methodology integrating Density Functional Theory (DFT) to investigate the photophysical properties of the 2HOE molecule. Our analysis of its geometry revealed critical structural features impacting orbital overlap and charge transfer absorption, emphasizing the significance of precise distances and angles. Moreover, the investigation of Frontier Molecular Orbital (FMO) energy gaps provided valuable insights into the compound chemical reactivity and stability. Notably, a lower FMO energy gap indicates heightened chemical reactivity and reduced kinetic stability, of the molecule. Overall, this thorough theoretical exploration of the 2HOE molecule contributes significantly to advancing our understanding of its behavior in various environments, thereby facilitating the exploration of its potential biological properties.

5.0 References

1. Howlader N, Noone AM, Krapcho M, Miller D, Bishop K, Kosary CL. American Cancer Society Cancer Facts and Figures 2018. Atlanta: American Cancer Society; 2018.
2. Amin KM, Eissa AA, Abou-Seri SM, Awadallah FM, Hassan GS. Synthesis and biological evaluation of novel coumarin-pyrazoline hybrids endowed with phenylsulfonyl moiety as antitumor agents. Eur J Med Chem. 2013; 60:187-98. https://doi.org/10.1016/j.ejmech.2012.12.004
3. Miladiyah I, Jumina J, Haryana SM, Mustofa M. Biological activity, quantitative structure-activity relationship analysis, and molecular docking of xanthone derivatives as anticancer drugs. Drug Des Devel Ther. 2018; 149-58. https://doi.org/10.2147/DDDT.S149973
4. Emami S, Dadashpour S. Current developments of coumarin-based anti-cancer agents in medicinal chemistry. Eur J Med Chem. 2015; 102:611-30. https://doi.org/10.1016/j.ejmech.2015.08.033
5. Jain PK, Joshi H. Coumarin: chemical and pharmacological profile. J Appl Pharm Sci. 2012; 236-40.
6. Lacy A, O'Kennedy R. Studies on coumarins and coumarin-related compounds to determine their therapeutic role in the treatment of cancer. Curr Pharm Des. 2004; 10(30):3797-811. https://doi.org/10.2174/1381612043382693
7. Rohini KSP, Srikumar PS. Therapeutic role of coumarins and coumarin-related compounds. J Thermodyn Catal. 2014; 5(2):1-3.
8. Thakur A, Singla R, Jaitak V. Coumarins as anticancer agents: A review on synthetic strategies, mechanism of action, and SAR studies. Eur J Med Chem. 2015; 101:476-95. https://doi.org/10.1016/j.ejmech.2015.07.010
9. Ghantwal SR, Samant SD. Claisen rearrangement of 3-bromo-, 3,6-dibromo-, 3,8-dibromo- and 8-iodo/aminomethyl/acetyl-7-allyloxy-4-methylcoumarins. 1999. https://doi.org/10.1002/chin.200017048
10. Majumder PL, Majumder S. Further evidence for the mechanism of formation of coumarin by Perkin reaction from salicylaldehyde and a novel synthesis of 1,1-diphenyl-2 (2'-hydroxyphenyl) ethene from O-α,α-diphenylacetylsalicylaldehyde with Et3N. Eur J Med Chem. 1993; 28:572-8.
11. Gedeck P, Kramer C, Ertl P. Computational analysis of structure-activity relationships. Prog Med Chem. 2010; 49:113-60. https://doi.org/10.1016/S0079-6468(10)49004-9
12. Piir G, Kahn I, García-Sosa AT, Sild S, Ahte P, Maran U. Best practices for QSAR model reporting: physical and chemical properties, ecotoxicity, environmental fate, human health, and toxicokinetics endpoints. Environ Health Perspect. 2018; 126(12):126001. https://doi.org/10.1289/EHP3264
13. Taboureau O, Baell JB, Fernández-Recio J, Villoutreix BO. Established and emerging trends in computational drug discovery in the structural genomics era. Chem Biol. 2012; 19(1):29-41. https://doi.org/10.1016/j.chembiol.2011.12.007

14. Miteva MA, Villoutreix BO. Computational biology and chemistry in MTi: emphasis on the prediction of some ADMET properties. Mol Inform. 2017; 36(10):1700008. https://doi.org/10.1002/minf.201700008
15. Savanur HM, Pawashe GM, Kim KM, Kalkhambkar RG. Synthesis and molecular modelling studies of coumarin- and 1-aza-coumarin-linked miconazole analogues and their antifungal activity. Chem Select. 2018; 3(33):9648-53. https://doi.org/10.1002/slct.201801408
16. Frisch MJ, Trucks GW, Schlegel HB, Scuseria GE, Robb MA, Cheeseman JR, *et al.* Gaussian 09, Revision B.01. Wallingford, CT: Gaussian, Inc; 2010.
17. Raghavachari K. Density-functional thermochemistry. III. The role of exact exchange. Becke AD. J Chem Phys. 2000; 98. https://doi.org/10.1007/978-3-662-10421-7_60
18. Shirley WA, Hoffmann R, Mastryukov VS. An approach to understanding bond length/bond angle relationships. J Phys Chem. 1995; 99(12):4025-33. https://doi.org/10.1021/j100012a024
19. Tsuzuki S, Uchimaru T, Tanabe K, Yliniemela A. Comparison of atomic charge distributions obtained from different procedures: basis set and electron correlation effects. J Mol Struct: Theochem. 1996; 365(2-3):81-8. https://doi.org/10.1016/0166-1280(96)04500-9
20. Jain R, Jain VK, Chandra AR, Jain V, Lakshmi N. Study of the electronic structure, magnetic and elastic properties and half-metallic stability on variation of lattice constants for CoFeCr Z (Z= P, As, Sb) Heusler alloys. J Supercond Nov Magn. 2018; 31:2399-409. https://doi.org/10.1007/s10948-017-4460-3
21. Zara Z, Iqbal J, Ayub K, Irfan M, Mahmood A, Khera RA, *et al.* A comparative study of DFT calculated and experimental UV/Visible spectra for thirty carboline and carbazole based compounds. J Mol Struct. 2017; 1149:282-98. https://doi.org/10.1016/j.molstruc.2017.07.093
22. Nayak R, Tarkes DP, Satapathy A. A computational and experimental investigation on thermal conductivity of particle reinforced epoxy composites. Comput Mater Sci. 2010; 48(3):576-81. https://doi.org/10.1016/j.commatsci.2010.02.025
23. Yerrasani R, Karunakar M, Dubey R, Singh AK, Nandi R, Singh RK, *et al.* Synthesis, characterization and photophysical studies of rare earth metal complexes with a mesogenic Schiff-base. J Mol Liq. 2016; 216:510-5. https://doi.org/10.1016/j.molliq.2016.01.052